

Low-temperature SOFCs based on $\text{Gd}_{0.1}\text{Ce}_{0.9}\text{O}_{1.95}$ fabricated by dry pressing

Changrong Xia, Meilin Liu*

School of Materials Science and Engineering, Georgia Institute of Technology, Atlanta, GA 30332-0245, USA

Received 9 April 2001; received in revised form 24 August 2001; accepted 27 August 2001

Abstract

Anode-supported solid oxide fuel cells (SOFCs) based on gadolinia-doped ceria (GDC, $\text{Gd}_{0.1}\text{Ce}_{0.9}\text{O}_{1.95}$) are fabricated by a simple and cost-effective dry-pressing process. With a composite anode consisting of NiO + 35 wt.% GDC and a composite cathode consisting of $\text{Sm}_{0.5}\text{Sr}_{0.5}\text{CoO}_3$ (SSC) and 10 wt.% GDC, the cells are tested at temperatures from 400 to 650°C. When humidified (3% H_2O) hydrogen is used as fuel and stationary air as oxidant, the maximum power densities are 145 and 400 mW/cm^2 at 500 and 600°C, respectively. Impedance analysis indicates that the performances of the SOFCs are determined essentially by the interfacial resistances below 550°C. Further, while the anodic polarization resistances are negligible, the cathodic polarization resistances are significant, suggesting that development of new cathode materials is especially important to SOFCs to be operated at low temperatures. © 2001 Elsevier Science B.V. All rights reserved.

Keywords: Solid oxide fuel cells; $\text{Gd}_{0.1}\text{Ce}_{0.9}\text{O}_{1.95}$; Dry pressing

1. Introduction

Solid oxide fuel cells (SOFCs) have a great potential to be the cleanest, most efficient, and versatile technologies for chemical-to-electrical energy conversion. While the existing SOFC technology has demonstrated much higher energy efficiency with minimal pollutant emission over conventional energy technologies, the cost of the current SOFC systems is still prohibitive for wide commercial applications. To be economically competitive, the cost of materials and fabrication must be dramatically reduced. One effective approach to cost reduction is to reduce the operating temperature so that interconnection, heat

exchanges, and structural components may be fabricated from relatively inexpensive metal components. The operating temperature can be reduced by decreasing the electrolyte thickness, by using electrolyte of high ionic conductivity at low temperatures, or by reducing electrode–electrolyte interfacial resistances [1,2]. Recently, considerable efforts have been directed to reduced-temperature SOFCs based on thin-film electrolyte of doped ceria. With a 30- μm -thick $\text{Gd}_{0.2}\text{Ce}_{0.8}\text{O}_{1.9}$ fabricated by multi-layer tape casting, Doshi et al. [3] reported a maximum power density of 140 mW/cm^2 at 500°C for a H_2 /air fuel cell. Single cells based on a thin-film electrolyte of stabilized zirconia coated with doped ceria by magnetron sputtering generated power densities up to 125 mW/cm^2 at 550°C with methane as fuel [4]. More recently, we have demonstrated maximum power densities of 188 at 500°C with humidi-

* Corresponding author. Tel.: +1-404-894-6114; fax: +1-404-894-9140.

E-mail address: meilin.liu@mse.gatech.edu (M. Liu).

fied hydrogen as fuel for a cell based on a 30- μm -thick $\text{Sm}_{0.2}\text{Ce}_{0.8}\text{O}_{1.9}$ fabricated by screen printing [5].

To significantly reduce the cost of fabrication, we have studied dry pressing for fabrication of dense ceramic membranes on porous substrates. Compared with physical or chemical vapor deposition or other extensively studied methods for film preparation [1], dry pressing is simple, reproducible, and very cost-effective. This technique has been widely used in laboratory and industry to make parts thicker than 0.5 mm. Single cells based on GDC electrolyte membranes as thin as 8 μm have been successfully fabricated using dry pressing in our laboratory and the detailed fabrication is as described elsewhere [6,7]. In this paper, we report our findings in characterization of a single cell based on a $\text{Gd}_{0.1}\text{Ce}_{0.9}\text{O}_{1.95}$ (GDC) electrolyte fabricated by dry pressing. The observed power densities and the interfacial resis-

tances of a dry-pressed SOFC represent a significant progress in development of low-temperature SOFCs.

2. Experimental

The GDC ($\text{Gd}_{0.1}\text{Ce}_{0.9}\text{O}_{1.95}$) powder was prepared using a glycine–nitrate process [8–10]. Stoichiometric amounts of $\text{Ce}(\text{NO}_3)_3$ and $\text{Gd}(\text{NO}_3)_3$ were dissolved in distilled water, to which glycine was added. The mixture was heated on a hot plate, evaporated to a brown-red gel, ignited to flame, and finally converted to pale-yellow ash, which was then fired at 600°C for 2 h to form $\text{Gd}_{0.1}\text{Ce}_{0.9}\text{O}_{1.95}$ with fluorite structure, as examined by X-ray diffraction (Scintag X1). The powder has a foamed structure with extremely low density as characterized using a scanning electron microscope (SEM, Hitachi S-800). The powder was added to a hardened metal die in which

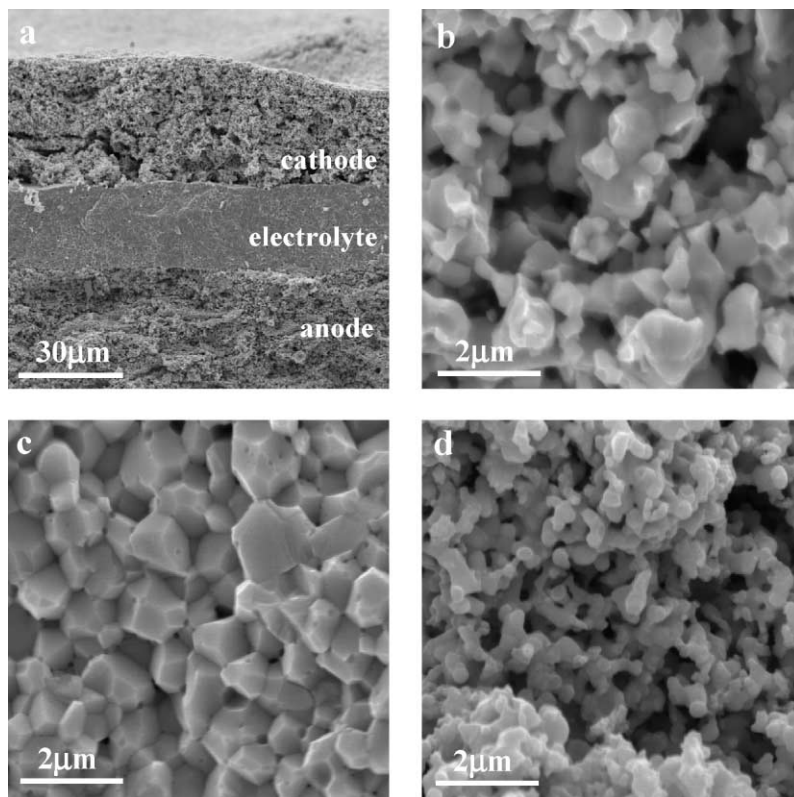


Fig. 1. Cross-sectional views (SEM micrographs) of (a) a single cell, (b) the porous Ni-GDC anode, (c) the dense GDC electrolyte, and (d) the porous SSC-GDC cathode.

NiO and GDC powder (NiO/GDC = 65:35) was prepressed under 200 MPa as substrate. The GDC powder and the substrate were then copressed at 250 MPa to form a green bilayer and subsequently cofired at 1350°C in air for 5 h to densify the GDC film [6,7]. The diameters of the green and the sintered pellets were 25 and 21 mm, respectively. The film thickness can be easily controlled with the amount of GDC powder [6,7]. The porosity of the anode before and after reduction was measured using a standard Archimedes method. Slurry consisting of $\text{Sm}_{0.5}\text{Sr}_{0.5}\text{CoO}_3$ (SSC, prepared by glycine–nitrate method), 10 wt.% GDC, and a Heraeus binder (V-006) was then applied to the electrolyte by screen printing, which was then fired at 950°C in air for 4 h to form a porous cathode. The porosity of the cathode was estimated by the weight, the area, and the thickness as determined by SEM of the cathode layer. The Ag reference electrode ($1 \times 10 \text{ mm}^2$) was prepared by painting a silver paste (Heraeus 8710) on the cathode side electrolyte, about 2 mm away from the edge of cathode, and subsequently firing at 700°C for 1 h [11].

The single cell was sealed on an alumina tube with a silver paste (Heraeus, C8710). Electrochemical characterizations were performed at temperatures from 400 to 650°C under ambient pressure. Fuel-cell performances were measured with an EG&G Potentiostat/Galvanostat (Model 273A) interfaced with a computer. Humidified (3% H_2O) hydrogen was used as fuel and stationary air as oxidant. The impedances were measured typically in the frequency range from 0.1 Hz to 100 kHz using an EG&G lock-in amplifier (model 5210) and the Potentiostat/Galvanostat interfaced with a computer.

3. Results and discussion

3.1. Microstructure of the cell

Shown in Fig. 1 are the cross-sectional SEM micrographs of each cell component. The electrolyte layer is about 26- μm thick, the grain size varies from 1 to 2 μm , and the relative density is

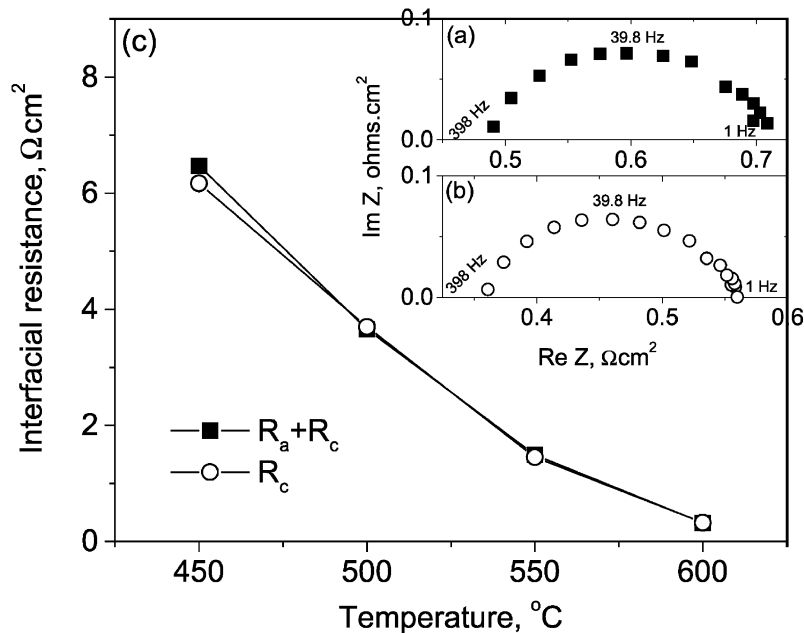


Fig. 2. Impedance spectra of a single cell as measured using (a) a two-electrode configuration (total impedance of the whole cell) and (b) a three-electrode configuration (WE: cathode, CE: anode, RE: Ag electrode adjacent to cathode). The interfacial resistances obtained from impedance spectra at different temperatures are shown in (c).

about 92%, as estimated from the dimensions of the film and the amount of GDC powder used to make the film. Some isolated defects such as small voids were observed under SEM investigation. However, no cross-membrane cracks or pinholes were observed. The cathode layer, consisting of sub-micron grains, has an average thickness of 30 μm and a porosity of about 40%. The thickness of the porous anodes varied from 0.5 to 0.7 mm whereas the porosities of the anodes were about 12% and 36%, respectively, before and after the NiO was reduced to Ni. The volume fractions of SDC and nickel in the reduced anode were estimated to be about 30% and 34%, respectively.

3.2. Interfacial resistance of anode

Shown in Fig. 2(a) is a typical impedance spectrum of a single cell measured under open circuit conditions at 600°C using a two-electrode configuration. The intercept with the real axis at high frequencies represents the resistance of the electrolyte whereas the diameter of the depressed semicircle corresponds to the impedance of the two interfaces: the cathode–electrolyte interface (R_c) and the anode–electrolyte interface (R_a). The interfacial resistance includes the contact resistance between the electrode and the electrolyte as well as the resistance to the electrochemical processes such as charge

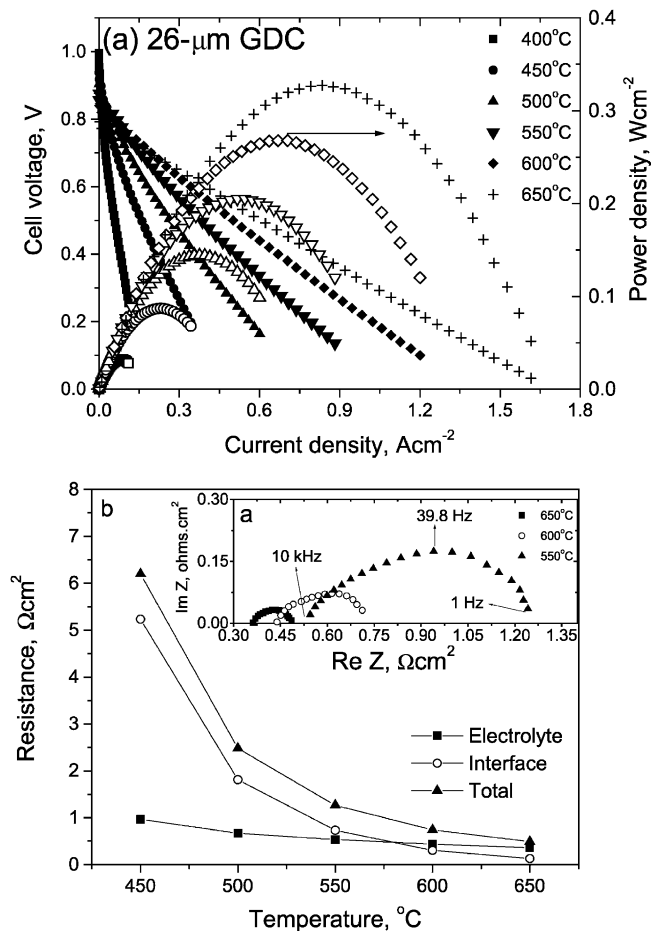


Fig. 3. (a) The I - V curves (solid symbols) and the corresponding power densities (open symbols) for a cell based on a 26- μm -thick GDC membrane, when humidified hydrogen was used as fuel and stationary air as oxidant. (b) Impedance spectra (the insert) of the cell as measured under open-circuit conditions at 550, 600 and 650°C, and the electrolyte resistances, the interfacial polarization resistances and the total resistances as determined from the impedance spectra.

transfer and mass transfer. To separate the cathodic from the anodic interfacial resistance, a three-electrode configuration was used in the impedance measurements on the same cell. Shown in Fig. 2(b) is a typical impedance spectrum at 600°C under open circuit conditions using the cathode as the working electrode (WE), the anode as the counter electrode (CE) and the Ag electrode (adjacent to the cathode) as the reference electrode (RE). The intercept, with the real axis at high frequencies, represents part (about 50%) of the electrolyte resistance whereas the

diameter of the depressed semicircle corresponds to the resistance of the cathode–electrolyte interface (R_c). The use of the Ag reference electrode in the impedance measurement had successfully eliminated the influence of the anode–electrolyte interface on the impedance spectra. Further, when the WE and the CE were switched, i.e. the WE was connected to the anode and the CE was connected to the cathode, the impedances of the anode–electrolyte interface were obtained. In this case, however, the interfacial resistances were so small that they came to a point

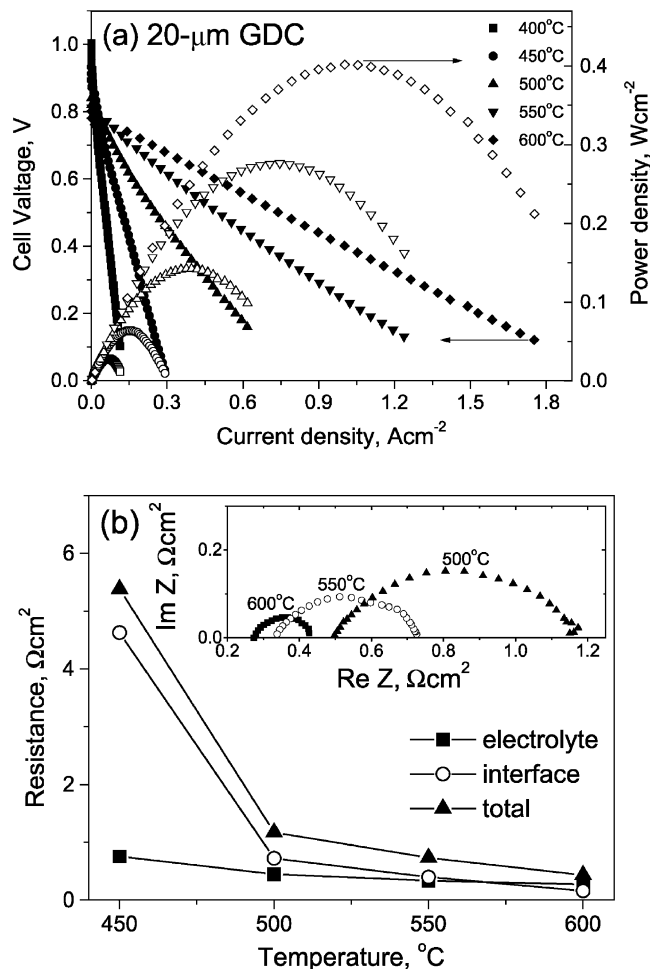


Fig. 4. (a) The I - V curves (solid symbols) and the corresponding power densities (open symbols) for a cell based on a 20- μm -thick GDC membrane when humidified hydrogen was used as fuel and stationary air as oxidant. (b) Impedance spectra (the insert) of the single cell as measured under open-circuit conditions at 500, 550 and 600°C, and the electrolyte resistances, the interfacial polarization resistances and the total resistances as determined from the impedance spectra.

implying that the anode–electrolyte interfacial impedances were negligible. Shown in Fig. 2(c) are the cathode–electrolyte interfacial resistances (R_c) and the total interfacial resistances ($R_c + R_a$) as determined from impedance spectra similar to those shown in Fig. 2(a) and (b) measured at different temperatures. Clearly, the interfacial resistances are dominated by the cathode–electrolyte interface and the resistances of the anode–electrolyte are negligible under the conditions studied.

3.3. Cell performance

Shown in Fig. 3(a) are the cell voltages and power densities for a single cell based on a 26- μm -thick GDC electrolyte membrane; the cross-sectional view of the cell is shown in Fig. 1. Each datum point was recorded about 30 min after the cell reached the steady state. An open-circuit voltage (OCV) of 1.01 V was observed at 400°C, indicating that the electronic conductivity of GDC was insignificant and the hydrogen permeation through the electrolyte membrane or the seals was negligible. However, the observed OCV decreased with temperature to 0.92 V at 500°C and 0.85 V at 600°C. This is due possibly to some leakage through silver seals. Nevertheless, the cell generated maximum power densities of 145, 205, 270 and 330 mW/cm^2 at 500, 550, 600 and 650°C, respectively. Shown in Fig. 3(b) are several impedance spectra of the cell measured under open-circuit conditions and the interfacial polarization resistances, electrolyte resistances, and total resistances of the cell as determined from the impedance spectra. It is immediately clear that the performance of the cell is influenced by the interfacial resistances, especially at temperatures below 550°C, where the cell performance is essentially determined by the interfacial resistances. As mentioned earlier, the resistances of the cathode–electrolyte interface are much greater than those of the anode–electrolyte interface. The anode–electrolyte interfacial resistances were negligible (or within experimental error) and the observed total interfacial resistances were due virtually to the cathode–electrolyte interfacial polarization.

Shown in Fig. 4(a) are the I – V curves and the corresponding power densities of another cell with

a 20- μm -thick GDC membrane as electrolyte. The resistances of the electrolyte and interfaces are shown in Fig. 4(b). A direct comparison in performance of the two cells is shown in Fig. 5. Above 500°C, the power densities of the cell with the thinner (20 μm) electrolyte were much greater than those of the cell with the thicker (26 μm) electrolyte because the total resistance of the cell were determined primarily by the electrolyte resistances, as shown in Fig. 5(b). The effect is more pronounced at higher temperature. Maximum power densities of 270 and 400 mW/cm^2 were achieved with the thinner electrolyte at 550 and 600°C, respectively. Below 500°C, however, the maximum power density of the two cells are essentially the same (Fig. 5(a)) because the total resistance of the cells were determined primarily by the interfacial resistances as shown in Fig. 5(b).

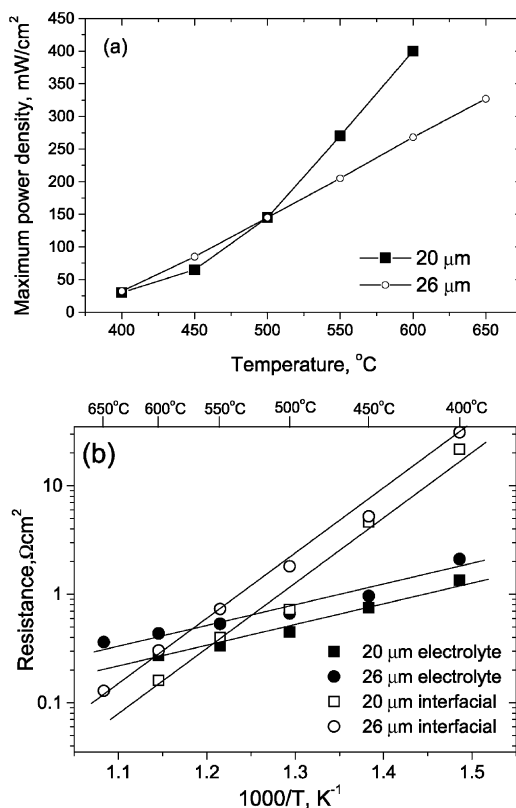


Fig. 5. The maximum power densities (a) and electrolyte and interfacial resistances (b) of two cells with different electrolyte thickness (20 and 26 μm).

Also, it is clearly seen from Figs. 3(b) and 4(b) that the ratio of interfacial resistance to electrolyte resistance increased dramatically as the operating temperature was reduced, implying that the performance of the SOFCs to be operated at low temperatures depends critically on the interfacial resistance. Accordingly, the development of catalytically active electrodes and interfaces is critical to successful development of SOFCs to be operated at low temperatures ($< 600^{\circ}\text{C}$). Mesoporous mixed-conducting electrodes and nanostructured interfaces may significantly improve the performance of low-temperature SOFCs.

4. Conclusions

GDC ($\text{Gd}_{0.1}\text{Ce}_{0.9}\text{O}_{1.95}$) films were successfully fabricated by a simple, cost-effective dry-pressing process. SOFCs based on GDC films were tested from 400 to 650°C with humidified hydrogen as fuel. Maximum power densities of 145 and $400\text{ mW}/\text{cm}^2$ were achieved at 500 and 600°C , respectively. Below 550°C , the fuel cell performances are essentially determined by the interfacial resistance of cathode–electrolyte interface, implying that development of catalytically active cathodes and fabrication processes are critical to the development of high-performance SOFCs to be operated below 600°C .

Acknowledgements

This work was supported by the National Science Foundation under Award No. CTS-9819850 and by Oak Ridge National Laboratory (ORNL). ORNL is operated by UT-Battelle, LLC for the US Department of Energy under contract DE-AC05-00OR22725.

References

- [1] J. Will, A. Mitterdorfer, C. Kleinogel, D. Perednis, L.J. Gauckler, *Solid State Ionics* 131 (2000) 79.
- [2] J.P.P. Huijsmans, F.P.F. van Berkei, G.M. Christic, *J. Power Sources* 71 (1998) 107.
- [3] R. Doshi, V.L. Richards, J.D. Carter, X. Wang, M. Krumpelt, *J. Electrochem. Soc.* 146 (1999) 1273.
- [4] E.P. Murray, T. Tsai, S.A. Barnett, *Nature* 400 (1999) 649.
- [5] C.R. Xia, F.L. Chen, M.L. Liu, *Electrochem. Solid-State Lett.* 4 (2001) A52–A54.
- [6] C.R. Xia, M.L. Liu, Provisional patent application filed on Feb 2001.
- [7] C.R. Xia, M.L. Liu, *J. Am. Ceram. Soc.* 84 (2001) 1903.
- [8] L.A. Chick, L.R. Pedersen, G.D. Maupin, J.L. Bates, L.E. Thomas, G.J. Exarhos, *Mater. Lett.* 10 (1990) 6.
- [9] N.J. Hess, G.D. Maupin, L.A. Chick, D.S. Sunberg, D.E. McCreedy, T.R. Armstrong, *J. Mater. Sci.* 29 (1994) 1873.
- [10] M.W. Murphy, T.R. Armstrong, P.A. Smith, *J. Am. Ceram. Soc.* 80 (1997) 165.
- [11] S. Wang, X. Lu, M. Liu, *J. Solid State Electrochem.* 5 (6) (2001) 375.